

Simple model for coupled magnetic and quadrupolar instabilities in uranium heavy-fermion materials

V. L. Líbero

Departamento de Física e Ciência dos Materiais, Instituto de Física e Química de São Carlos, Universidade de São Paulo, 13560 São Carlos, São Paulo, Brazil

D. L. Cox

Department of Physics, Ohio State University, Columbus, Ohio 43210

(Received 8 September 1992; revised manuscript received 19 March 1993)

We present a mean-field calculation of the phase diagram of a simple model of localized moments, in the hexagonal uranium heavy-fermion compounds. The model considers a non-Kramers quadrupolar doublet ground state magnetically coupled with a singlet excited state, favoring in-plane van Vleck magnetism, as has been conjectured for UPt_3 . The Hamiltonian that defines the model is Heisenberg-like in both magnetic and quadrupolar moments. No Kondo-effect physics is included in the calculations. Among our main results are (i) for zero intersite quadrupolar coupling, the magnetic order is achieved by a first-order transition above a critical intersite magnetic coupling value, which becomes second order at higher coupling strengths (ii) for finite intersite quadrupolar coupling, at temperatures below a second-order quadrupolar ordering transition, the minimal magnetic coupling value is increased, but (a) the magnetic ordering temperature is enhanced above this value, and (b) the ordering of first- and second-order transitions in the phase diagram is reversed. By considering the general structure of the Ginsburg-Landau free energy, we argue that the Kondo effect will not modify the shape of the phase diagram, but will modify the quantitative values at which transitions occur.

I. INTRODUCTION

The unusual commensurate, reduced-moment-magnetic order present in heavy-electron superconductors such as UPt_3 [and its related alloys $U(Pt_{1-x}, Pd_x)_3$ and $(U_{1-x}, Th_x)Pt_3$], URu_2Si_2 , and UPd_2Al_3 has so far resisted explanation in any simple terms. It is difficult to believe the small moment order represents itinerant spin-density wave formation, since, for example, UPt_3 displays no appropriate nesting features on the Fermi surface at the appropriate antiferromagnetic wave vector. It is difficult to account for the order in terms of frustration effects since the ordered structures are remarkably simple. In the case of URu_2Si_2 , moreover, there is evidence¹ that the magnetic order parameter is not the "primary" one, in the sense that despite the large entropy involved in the 17.5 K magnetic transition (the entropy involved is larger than in the 1.2 K superconducting transition) the effective moment is too small to be consistent with the size of the ordered moment. Indeed, it has been suggested^{2,3} that some other "hidden" order drives the transition (such as quadrupoles). Indeed, as noted elsewhere,⁴ the absence of a divergence in the ^{29}Si spin lattice relaxation rate⁵ at the transition suggests that it is nonmagnetic in origin. UPd_2Al_3 has a complex phase diagram, with a second-order transition at 14.5 K and an apparent first-order transition at 12.5 K.⁹ The higher transition is weakly dependent upon field up to ~ 8 T, while the second transition is rapidly suppressed by field. Hence, the higher-temperature transition does not behave like that of a conventional antiferromagnetic state.

Recent theoretical developments coming from different directions altogether make it prudent to consider quadrupolar (and octupolar) ordering possibilities in these materials: it has been noted that the quadrupolar Kondo model believed to be previously restricted to cubic uranium based materials is in fact possible for hexagonal (UPt_3) and tetragonal (URu_2Si_2) materials as well.⁶ In this model the heavy fermions arise from local uranium quadrupole moments associated with ground crystal-field doublets quenched by (predominantly) the orbital motion of itinerant electrons. Thus, the low lying degrees of freedom may be essentially quadrupolar.

The relevance of the quadrupolar Kondo model to this class of materials has been put on firmer footing by the discovery of the cubic material $Y_{1-x}U_xPd_3$ (Ref. 7) and $Th_{1-x}U_xRu_2Si_2$,⁸ which appear to display a dilute limit quadrupolar Kondo effect. Moreover, all known heavy-fermion superconductors possess the appropriate symmetry groups to yield a quadrupolar Kondo effect or magnetic two-channel Kondo effect ($CeCu_2Si_2$),⁶ a point bolstered by the recent discovery of two hexagonal heavy, electron superconductors (UPd_2Al_3 and UNi_2Al_3) which also possess magnetic order.⁹

In the quadrupolar Kondo picture, a context for weak moment magnetic order can arise naturally from two distinct sources. (i) For cubic symmetry, all magnetic character is in excited states, and for hexagonal and tetragonal symmetry, in-plane magnetic character is in excited states. Thus, the magnetic response is van Vleck in character yielding a built-in stability against magnetic ordering and a region of weak moment order. The same is true

for in-plane magnetic moments in hexagonal and tetragonal symmetry. (ii) For hexagonal and tetragonal symmetry, the c -axis character of the local uranium doublets is weakly magnetic, but primarily octupolar.

In this paper, we shall focus our attention on (i), with the particular goal of examining how quadrupolar order can induce or at least enhance magnetic ordering tendencies. While it is well known that quadrupolar order will always be induced as a secondary-order parameter at a magnetic transition, it seems to be less well known, at least in the heavy-fermion field, for magnetic order to be induced or enhanced by the coupling to quadrupolar degrees of freedom. Such physics is known in UO_2 , for example, where the antiferromagnetic phase transition is first order due to a coupling between magnetic and quadrupolar order parameters.¹⁰

We have performed mean-field calculations on a simple model of potential relevance to the hexagonal uranium heavy-fermion superconductors. In this model, each uranium ion possesses a doublet quadrupolar ground state magnetically coupled to an excited singlet state. The uranium ions are placed on a lattice with the structure of UPt_3 (though the point symmetry is taken to be D_{6h} rather than D_{3h}). The results will also be relevant to the hexagonal structure of UPd_2Al_3 and tetragonal structure of URu_2Si_2 , given that the crystal-field level scheme can be essentially similar. We then turn on nearest-neighbor in-plane and out-of-plane quadrupolar and magnetic coupling and study the resulting phase diagram. We find a rich structure, ranging from van Vleck magnetism with a tricritical point and critical exchange strength to alternately suppressed and enhanced magnetic order below a second-order quadrupolar transition. We discuss the phase diagram using both the full mean-field calculations and Landau theory in regions of validity. We stress that the topology of the phase diagram is unlikely to be altered by (i) inclusion of two-channel Kondo effect physics and (ii) fluctuations near the tricritical point. The former effect simply renormalizes the parameters of the Landau free energy whose structure is fixed by symmetry considerations alone. The latter produces logarithmic corrections to the singular behavior near the tricritical point, and may alter the value of couplings needed to produce the tricritical point, but does not alter the topology. We briefly discuss the connection of our model to the more widely studied Blume-Emery-Griffiths model, which produces similarly rich phase diagrams.¹¹

While the model does not produce a full explanation of the ordering in bulk UPt_3 (for which the specific heat shows no transition and the neutron elastic scattering peaks are not true resolution limited Bragg peaks) it may be of relevance to the Pd and Th doped alloys, to URu_2Si_2 , and to the new hexagonal superconductors. In any case, it represents the beginning of an alternative view of collective phenomena in the heavy-fermion materials which may ultimately provide a unifying view of the heavy-fermion state, superconductivity, and magnetism.

The outline of the paper is as follows. Section II provides an overview of the model. Section III develops the mean-field approximation to this model. Section IV

discusses our results in terms of Landau theory, paying special attention to the role of the orientation dependent coupling between quadrupolar and magnetic order parameters. Finally, in Sec. V we conclude and point out explicit experimentally relevant features of our model.

II. MODEL

In Sec. II A we write a single-site Hamiltonian, coupling the quadrupolar moment of the ground state of the uranium-ion with the electric-field gradient and the magnetic moment with an applied magnetic field. In the next section we introduce intersite coupling of the XY -model form for both quadrupolar and magnetic degrees of freedom. Within the mean-field approximation that Hamiltonian is equivalent to that of Sec. II A, but with coupling coefficients which depend self-consistently on the mean magnetic and quadrupolar moments.

A. Single-site Hamiltonian

Having in mind the motivations given in Sec. I, we define a single-site model in which the uranium ion has a non-Kramers quadrupolar doublet ground state magnetically coupled only with an excited state. Such a crystal-field scheme may arise for a U^4 , $5f^2$, $J=4$ at a site of hexagonal symmetry. Figure 1 defines the level structure of the model, where the doublet $|E_{\pm}\rangle$ and the singlet $|B\rangle$ are defined by

$$|E_{\pm}\rangle = u|\pm 4\rangle + v|\mp 2\rangle, \quad (1)$$

and

$$|B\rangle = \frac{|3\rangle + |-3\rangle}{2}, \quad (2)$$

where $|m\rangle$ are the eigenstates of the z component of the total angular momentum J . u and v are constants. The relevant matrix elements for the model we are defining are

$$\langle B|J_{\pm}|E_{\mp}\rangle = 2u + \sqrt{7}v \equiv a \quad (3)$$

and

$$\langle E_{\pm}|J_{\pm}^2|E_{\mp}\rangle = 2\sqrt{7}v \equiv b. \quad (4)$$

Since $u^2 + v^2 = 1$, the constants a and b defined here are not independent.

The other $J=4$ multiplet levels are not considered, so the model will be restricted to temperatures less than or

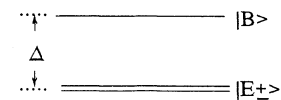


FIG. 1. Level structure of the model considered in this work. The doublet ground-state $|E_{\pm}\rangle = u|\pm 4\rangle + v|\mp 2\rangle$ is magnetic coupled to a singlet excited-state $\sqrt{2}|B\rangle = |3\rangle + |-3\rangle$, which has energy Δ . Here $|m\rangle$ is the eigenstate of the z component of the total angular momentum $J=4$. The other D_{6h} crystal-field levels are not included, thus restricting the model to temperatures less than Δ .

equal to the first excitation energy Δ . It is clear from the level structure considered that this model favors in-plane van Vleck magnetism, and c -axis Pauli magnetism, as has been conjectured for UPt_3 .⁶ The motivation for focusing on the doublet level is that it is the only degenerate level in hexagonal symmetry for U^{4+} ions, and we desire the internal degrees of freedom associated with the doublet level to allow for the Kondo effect. The formation of the many-body Abiksov-Suhl-Kondo resonance is the basic paradigm for the source of heavy fermions in these materials.

The doublet ground state corresponds to the E_2 representation of the point group D_{6h} , where the eigenfunctions transform like $x^2 - y^2$ and xy . This doublet has magnetic character along the c axis, but only in-plane quadrupolar tensors may couple the doublet levels together. This implies we can have a quadrupolar Kondo effect. Using the Stevens operator representation,¹² the corresponding quadrupolar operators are (proportional to) $Q_{xx} = -Q_{yy} = J_x^2 - J_y^2$ and

$$Q_{xy} = Q_{yx} = (J_x J_y + J_y J_x) / 2 .$$

The magnetic moment operator is $\mathbf{M} = g_J \mu_B \mathbf{J}$, where $g_J = \frac{4}{5}$ and μ_B is the Bohr magneton. The doublet is connected by J_x , and J_y to the excited $|B\rangle$ singlet. (Note that while the actual point group at U sites in UPt_3 is D_{3h} , the allowed crystal-field spectrum is essentially identical to that of D_{6h} .)

A single-site Hamiltonian H is defined coupling the quadrupolar operators with an electric-field gradient $\nabla \mathbf{E}$ and coupling the magnetic moment with an external magnetic field \mathbf{H} at the uranium site:

$$H = H_0 - \mathbf{H} \cdot \mathbf{M} - \sum_{\alpha, \beta} (\nabla_{\alpha} E_{\beta}) \hat{Q}_{\beta\alpha} , \quad (5)$$

where H_0 is the Hamiltonian for the uranium ion in the presence of the crystal field only (see Fig. 1):

$$H_0 = \Delta |B\rangle \langle B| . \quad (6)$$

We are measuring energies from the doublet ground state $|E_{\pm}\rangle$.

For in-plane \mathbf{H} and \mathbf{E} , the Hamiltonian equation (5) is written as

$$H = H_0 + AJ_+ + BJ_+^2 + \text{H.c.} , \quad (7)$$

where

$$A = -(g_J \mu_B / 2) (H_x - iH_y) \quad (8)$$

and

$$B = -(\lambda / 2) (\partial_{xx} E - \partial_{yy} E - 2i \partial_{xy} E) . \quad (9)$$

The diagonalization of this Hamiltonian shows that there is a crossing of levels depending upon \mathbf{H} and \mathbf{E} and an interplay between the field gradient and magnetic field which depends crucially on their orientation with respect to one another. In the model defined in the next section, the coefficients A and B are interpreted as molecular fields acting on the uranium sites. Since those molecular fields depend on the magnetic and quadrupolar moments,

a self-consistent calculation is required to obtain these moments at each temperature.

B. The intersite-coupling Hamiltonian

In order to determine the molecular fields \mathbf{H} and \mathbf{E} present in Eq. (5) we have used a model Hamiltonian which is Heisenberg-like in the magnetic moments as well as in the quadrupolar moments, defined by

$$H = H_0 - \sum_{\langle i, j \rangle} (I_m^{ab} \mathbf{M}_i \cdot \mathbf{M}_j + I_m^c \mathbf{M}_i \cdot \mathbf{M}_j + I_q^{ab} \text{Tr} \hat{Q}_i \cdot \hat{Q}_j + I_q^c \text{Tr} \hat{Q}_i \cdot \hat{Q}_j) , \quad (10)$$

where I_m^{ab} (I_m^c) is the coupling between the nearest-neighbor magnetic moments in the basal plane (c -axis direction) of the hexagonal lattice; I_q^{ab} (I_q^c) has the same meaning for the quadrupolar moments. Tr means trace over the product of the quadrupolar tensors.

We are interested in studying the antiferromagnetic order of the model defined by Eq. (10), so that the couplings I_m^{ab} and I_m^c are negative. Only ferroquadrupolar coupling I_q has been considered. We have examined the effect of a coupling of the form $\text{Tr} \mathbf{M}_i \cdot \hat{Q}_j \cdot \mathbf{M}_k$ in the Hamiltonian equation (10). It does not qualitatively change the mean-field phase diagram of the model since the couplings already present in Eq. (10) give rise to a term proportional to $M^2 Q$ in the free energy [see Eq. (20)]. Hence we will drop this coupling from the Hamiltonian. The calculations are restricted to the case when \mathbf{M} lies in x direction (that is, the case for UPt_3 , as shown by neutron-scattering data¹⁴), although it is possible to consider the general case.

C. Connection to Blume-Emery-Griffiths model

The Blume-Emery-Griffiths (BEG) model^{11,13} is widely studied as a source of tricritical phenomena suitable for describing, e.g., ^3He - ^4He mixtures and metamagnets such as DAG.¹⁶ In this model, every site has a spin-1 magnetic moment, and the Hamiltonian is

$$H_{\text{BEG}} = J \sum_{\langle ij \rangle} S_i^z S_j^z + K \sum_{\langle ij \rangle} (S_i^z)^2 (S_j^z)^2 + \Delta \sum_i (S_i^z)^2 . \quad (11)$$

Clearly, the J term gives nearest-neighbor magnetic coupling, the K term gives nearest-neighbor quadrupolar coupling, and the Δ term gives a crystal-field splitting of the type we are considering here. The key difference between H_{BEG} and the model we are considering is that the quantization axes are fixed in H_{BEG} such that the quadrupolar moment and magnetic moment are quantized in the same direction and the 3×3 mean-field Hamiltonian is diagonal. For a given set of parameters, our mean-field Hamiltonian is nondiagonal. We can, of course, diagonalize it, and thus we can find a set of J , K , and Δ for H_{BEG} appropriate to each set of parameters and each temperature in our Hamiltonian by matching the eigenvalues of each mean-field Hamiltonian. However, because of the arbitrary quantization axes in our model, *we cannot describe it by a single set of BEG parameters for all temperatures*. Hence our model is more general than the

BEG model, but the models share some common features, particularly the tricritical point.

III. MEAN-FIELD THEORY

A. Mean-field Hamiltonian

The mean-field approach consists of replacing the operators in the Hamiltonian by their mean values plus the respective fluctuations, and keeping the fluctuations only up to first order. Denoting the mean value of the magnetic and quadrupolar moment by $\bar{M} \equiv g_J \mu_B a \bar{m}$ and $\bar{Q} \equiv b \bar{q}$, respectively, where the matrix elements a and b are defined in Eqs. (3) and (4), the mean field applied to Eq. (10) results in

$$\frac{H}{\Delta} = \frac{H_0}{\Delta} - N(A\bar{m} + B\bar{q}) + 2 \sum_i (A m_i^x + B q_i^{xx}), \quad (12)$$

where N is the number of sites of the hexagonal lattice,

$$A = \frac{(I_M^{ab} + I_M^c) a^2}{\Delta} \bar{m} \equiv J_m \bar{m}, \quad (13)$$

and

$$B = -6 \frac{(I_Q^{ab} + I_Q^c) b^2}{\Delta} \bar{q} \equiv -6J_q \bar{q}. \quad (14)$$

The last equalities, Eqs. (13) and (14), define the dimensionless magnetic coupling J_m and the dimensionless quadrupolar coupling J_q , respectively. We are deliberately using the same notation A and B here as in Eqs. (8) and (9) since in both cases the meaning of those parameters

are the same, although in Eqs. (13) and (14) A and B depend on the order parameters \bar{m} and \bar{q} .

The site-independent terms of H are called the condensed energy; the other terms define a sum over an effective one-site Hamiltonian H_i , which can be written in terms of the components of the total angular momentum as

$$H_i = H_{0i} + A(J_{i+} + J_{i-}) + B(J_{i+}^2 + J_{i-}^2). \quad (15)$$

Diagonalizing H_i in the subspace defined by the electronic levels shown in Fig. 1 we find the following expression for the free-energy per site and in units of Δ :

$$f = -J_m \bar{m}^2 + 6J_q \bar{q}^2 - t \ln(e^{6\beta J_q \bar{q}^2} + 2e^{-\beta(1-6J_q \bar{q}^2)} \cosh \beta C) + t \ln(2 + e^{-\beta}), \quad (16)$$

where $\beta = 1/t$ is the inverse of the dimensionless temperature $t \equiv T/\Delta$. C is given by

$$C = \left[\left(\frac{1 + 6J_q \bar{q}}{2} \right)^2 + 2J_m^2 \bar{m}^2 \right]^{1/2}. \quad (17)$$

From the free energy, we obtain the following coupled equations for the order parameters \bar{m} and \bar{q} :

$$\bar{m} = -2 \frac{J_m \bar{m}}{C} \frac{\sinh \beta C}{\exp[\beta(1 - 18J_q \bar{q})/2] + 2 \cosh \beta C} \quad (18)$$

and

$$\bar{q} = \frac{1}{2} \frac{\cosh \beta C + (1 + 6J_q \bar{q})/(2C) \sinh \beta C - \exp[\beta(1 - 18J_q \bar{q})/2]}{\exp[\beta(1 - 18J_q \bar{q})/2] + 2 \cosh \beta C}. \quad (19)$$

Before solving Eqs. (18) and (19) numerically, we describe a few limits where it is possible to study these equations analytically. There is no solution other than the trivial $\bar{m} = 0$ and $\bar{q} = 0$ if $J_m < -\frac{1}{2}$ and $J_q = 0$. A pure magnetic phase ($\bar{m} \neq 0, \bar{q} = 0$) does not exist, but a pure quadrupolar phase ($\bar{m} = 0, \bar{q} \neq 0$) exists for $|J_m| < (1 + 3J_q)/2$ and $J_q \neq 0$. In that phase, for $T \ll \Delta$ one has $\bar{q} \approx 0.5 \tanh(6\beta J_q \bar{q})$, which implies the quadrupolar degrees of freedom are playing the role of a pseudospin $\frac{1}{2}$. In this regime, a second-order critical line appears at $t_{cq} \approx 3J_q$. The other regimes of Eqs. (18) and (19) are studied numerically. The next section discusses the phase diagram obtained by studying the stabilities of the solutions \bar{m} and \bar{q} for different temperatures and values of the coupling coefficients J_m and J_q .

B. Phase diagrams

Figure 2 shows the phase diagram of the model defined by Eq. (12). The main features of this diagram are the enhancement of the critical temperature and the interchange between first- and second-order transitions when the quadrupolar coupling J_q is introduced.

We first consider the case when $J_q = 0$. Both order parameters, \bar{m} and \bar{q} , are critical simultaneously and despite the fact that we do not have quadrupolar coupling in this case, the ground state described by the Hamiltonian H , Eq. (12), has quadrupolar degrees of freedom and for different temperatures the stability of this ground state against the intersite magnetic coupling causes the tricritical point (denoted by TP), separating the first- and second-order transitions. The coordinates of this tricritical point are $J_m = -1.05$ and $t_c = 0.300$. The line of second order is obtained from the limit \bar{m} and \bar{q} going to zero in Eqs. (18) and (19) and is given by

$$e^{\beta_c} = (J_m - \frac{1}{2}) / (J_m + 1).$$

Near this line \bar{m} follows the usual $(t_c - t)^{1/2}$ behavior characteristic of the order parameter in mean-field theory; \bar{q} is proportional to \bar{m}^2 , which is characteristic of the secondary order parameter. The first-order line extends from the tricritical point to $J_m = -\frac{1}{2}$; below this point no order is found for either \bar{m} or \bar{q} .

For nonzero J_q we have simultaneously first-order transitions for both order parameters only above the crit-

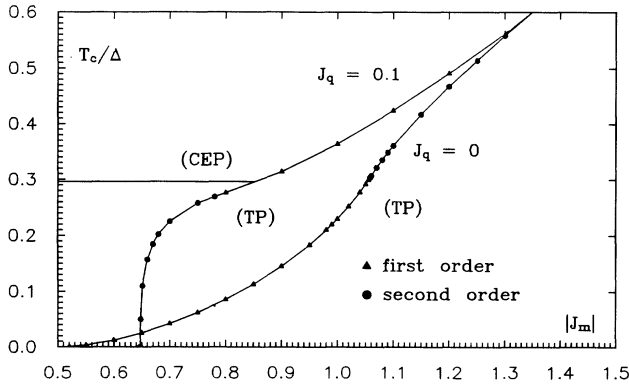


FIG. 2. Mean-field phase diagram of the model defined by the Hamiltonian, Eq. (12). J_m and J_q are the dimensionless magnetic and quadrupolar coupling between the nearest-neighbor sites, respectively, and $t_c \equiv k_B T_c / \Delta$ is the dimensionless critical temperature. At the right of the critical end point (denoted by CEP), both order parameters have the same critical temperatures. At the left, the transitions are separated into one pure second-order quadrupolar (horizontal straight line) and one pure first-order magnetic transition (dashed line). This last one ends at the tricritical point (denoted TP) where a line of second-order magnetic transition begins and ends at $t=0$ and $J_m = -0.5(1+3J_q)$. The quadrupolar coupling enhances the critical temperature t_c , increases the absolute value of the minimum magnetic coupling J_m necessary to have magnetic order, and reverses the nature of the phase transitions respect to the tricritical point.

ical end point, denoted by CEP in Fig. 2. Below this point the transitions are separated in one line of second-order purely quadrupolar transition at

$$t_{cq} = 6J_q / (2 + e^{-1/t_{cq}})$$

and another line of first-order purely magnetic transition. This latter line has a TP, becoming second-order below this point and finishing at $t=0$ and $J_m = -(1+3J_q)/2$; below this value of J_m one has only quadrupolar order. In Table I we have listed positions of the points CEP and TP for a few values of J_q . Figure 3 shows typical behavior of both order parameters with temperature, in different parts of the phase diagram.

Besides changing the values of the critical temperatures and separating the phases below the CEP, the intersite quadrupolar coupling has a more dramatic effect on the phase diagram, inverting the nature of the phases with respect to the TP: the first-order transition occurs below the TP when $J_q=0$, and exactly the opposite

TABLE I. Coordinates of the tricritical points (TP) and critical end points (CEP) in the phase diagram of Fig. 2, for different quadrupolar coupling J_q .

J_q	t_{TP}	$-J_m^{TP}$	t_{CEP}	$-J_m^{CEP}$
0.0	0.30	1.06		
0.05	0.12	0.64	0.14	0.70
0.1	0.27	0.79	0.29	0.83
0.2	0.52	1.01	0.55	1.10

occurs when $J_q \neq 0$. We believe this complicated effect of the indirect magnetic-quadrupolar coupling generated by the Hamiltonian equation (10) exists even for a very small quadrupolar coupling. This is confirmed by Landau's mean-field theory, which is discussed in Sec. IV.

C. Specific-heat jumps

Table II shows numerical calculations of the value of the specific-heat jumps, ΔC , for the second-order magnetization transitions for different quadrupolar coupling J_q . For zero J_q , ΔC is never less than 6 J/mol K. For nonzero J_q , ΔC is a very sensitive function of J_m , giving values of ΔC around 2 J/mol K for $J_q=0.05$, and $J_m = -0.6$, which is the experimental value of ΔC for the compound $U_{1-x}\text{Th}_x\text{Pt}_3$. For these J_m and J_q , and considering that the Néel temperature is equal to 6 K for this compound, the model also gives the value of energy splitting Δ of the crystal field as 70 K, which is the order of magnitude expected for this material. Naturally, we will have corrections to the specific-heat jump when including explicitly the interaction with the conduction-band electrons. If these corrections are not too large, the model shows that a very small quadrupolar coupling, about one order of magnitude smaller than the magnetic coupling, is necessary to obtain the magnitude of the specific-heat jump.

IV. LANDAU'S MEAN-FIELD THEORY

Contrary to the previous section, which treated the molecular-field-theory free energy exactly, we now want to use the Landau's mean-field theory, which is valid in the limit of small order parameters, i.e., near a second-order transition. This theory, although limited, can describe some of the features of the phase diagrams.

A. Free energy

The Landau's mean-field theory uses an approximation for the free energy, valid near the region where the order parameters \bar{m} and \bar{q} are small. Expanding the free energy given by Eq. (16) around $\bar{m}=0$ and $\bar{q}=0$ we have

$$f = \alpha_m \bar{m}^2 + \beta_m \bar{m}^4 + \gamma_m \bar{m}^6 + \alpha_q \bar{q}^2 + \beta_q \bar{q}^4 + \delta_{mq} \bar{m}^2 \bar{q} + \epsilon_{mq} \bar{m}^2 \bar{q}^2 + \dots, \quad (20)$$

where the coefficients are functions of the temperature t and of the couplings J_m and J_q . They are listed in Table III.

For $J_q=0$, only the three first terms on the right-hand side of Eq. (20) survive and the critical temperatures for second-order transitions are obtained from the equation $\alpha_m(t, J_m)=0$, whose solutions agree with the numerical results. The coefficient $\beta_m(t, J_m)$ is negative (positive) for temperatures less (greater) than 0.300 32, and γ_m is positive (negative) for temperatures less (greater) than 0.463 70, for all J_m . That means we have first (second) order for critical temperatures less (greater) than 0.300 32. The point where both coefficients, α_m and β_m , vanish simultaneously determines the tricritical point (TP) and that is at $t_{TP}=0.300 32$ and $J_m^{TP}=-1.071 40$,

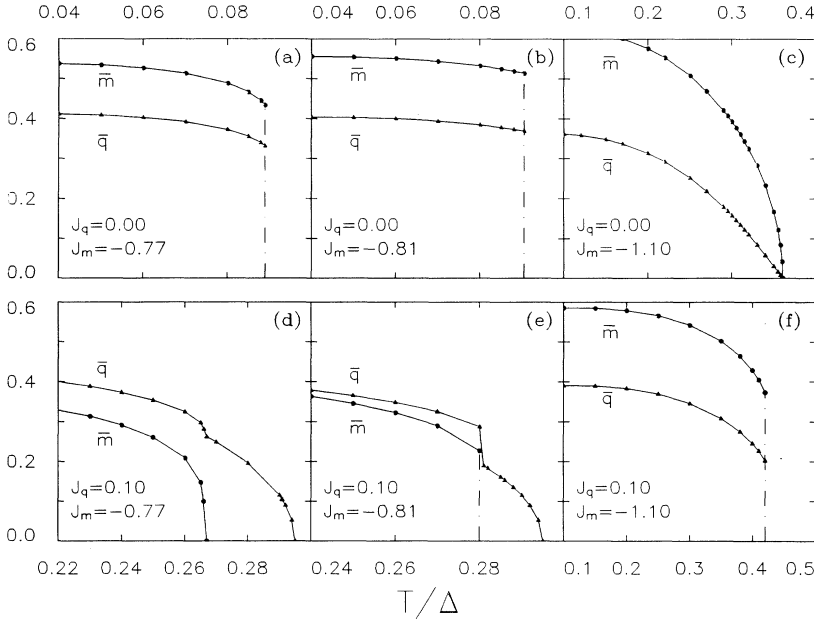


FIG. 3. Temperature dependence of the magnetic moment \bar{m} and quadrupolar moment \bar{q} , obtained from Eqs. (18) and (19). The temperatures on the x axis are measured in units of the crystal-field splitting Δ , and are not in the same scale; the units of all other quantities are defined in the text. For $J_q=0$, (a), (b), and (c), \bar{q} has the same critical temperatures as \bar{m} , and behaves like a secondary order parameter. For $J_q=0.1$, (d), (e), and (f), the quadrupolar transitions are separated from the magnetic ones, except for $|J_m| > |J_M^{\text{CEP}}| = 0.83$. For the same values of J_m the nature of the phase transitions changes according to whether J_q is present or not. No magnetic order is found without quadrupolar order.

also in agreement with the phase diagram Fig. 2.

The quadrupolar-coupling J_q complicates the analysis of the free energy Eq. (20). Now, the second-order magnetic transition (dashed line in Fig. 2) has nonzero quadrupolar order-parameter $\bar{q} = q_0$, so the free energy in fact should be written as

$$f = \alpha'_m(t, J_m, q_0)m^2 + \beta'_m(t, J_m, q_0)m^4 + \dots, \quad (21)$$

where q_0 is the equilibrium value of \bar{q} on the critical line ($\bar{m} = 0$), and is given by $q_0 = (-\alpha_q/2\beta_q)^{1/2}$. The critical temperature for the magnetic transition now is the solution of

$$\alpha'_m(t_c, J_m, q_0) \approx \alpha_m + \gamma q_0 + \delta q_0^2 + \dots = 0,$$

which gives t_c close to the numerical results, mainly near (but at left of) the tricritical point where q_0 is not too big. To calculate β'_m needs some care. Using the expansion (20) β'_m will have divergent terms at t_{cp} , which invalidate its expansion around the tricritical point since this point always occurs near t_{cp} . For $J_q = 0$ those terms do not exist and $\beta'_m = \beta_m$. We have computed β'_m through its definition:

$$\beta'_m = \frac{\partial^4 f}{\partial m^4} / 4!,$$

TABLE II. Specific-heat jumps ΔC of the second-order magnetic transitions on the phase diagram Fig. 2, for a few values of the quadrupolar coupling J_q . The magnetic coupling J_m are near the minimum value to give second-order transitions.

J_q	$-J_m$	ΔC
0.00	1.10	6.52
0.05	0.60	1.50
0.1	0.68	0.92
0.2	0.85	1.31

calculated at $\bar{m} = 0$ and $\bar{q} = q_0$, where q_0 is obtained from the numerical solution of Eqs. (18) and (19). β'_m showed no divergence and, although β_m can be negative, β'_m is positive for $t \leq t_{TP}$, which explains why we have a second-order transition when $J_q \neq 0$ instead of a first-order one when $J_q = 0$. Unfortunately, Landau's mean-field theory does not work well right above the TP since \bar{m} does not go to zero and, in fact, \bar{m} has a big jump at the critical temperature and so \bar{q} has a discontinuity at this line [see Fig. 3(e)]. For large J_m , however, the jumps in both order parameters at the critical line become small, thus the expansion (20) gives a reasonable description of the model in this limit.

We note that the enhancement of magnetic ordering by quadrupolar ordering for sufficiently high I_M can be qualitatively understood from the Landau free energy. The origin is the same third-order term in the free energy, which has a negative definite contribution to the energy since it depends upon the orientation of quadrupolar and magnetic order parameters (deriving from a $\mathbf{M} \cdot \hat{Q} \cdot \mathbf{M}$ term with full rotational symmetry retained). For fixed Q , this enhances the second-order magnetic transition temperature according to

$$T_M \rightarrow T_M + \frac{|\gamma_{mq}||Q|}{\partial \alpha_m / \partial T}, \quad (22)$$

TABLE III. Coefficients of the expansion of the free energy defined in Eq. (20). Here $d = (2e^{\beta/2} + e^{-\beta/2})^{-1}$.

$\alpha_m = -4dJ_m^2 \sinh(\beta/2) - J_m$
$\beta_m = 2d^2J_m^4[(2-\beta)e^\beta - 5\beta - 1 - e^{-\beta}]$
$\gamma_m = 8J_m^6(3\beta^2d^3 - 4d)\sinh(\beta/2) + 8J_m^6\beta d^2(5 + e^\beta)$
$\alpha_q = 6dJ_qe^{\beta/2}(2 + e^{-\beta} - 6J_q\beta)$
$\beta_q = 108d^2J_q^4\beta^3(4e^\beta - 1)$
$\delta_{mq} = 12dJ_m^2J_q[\beta e^{\beta/2} - 2\sinh(\beta/2)]$
$\epsilon_{mq} = 36d^2J_m^2J_q^2(4\beta e^{\beta/2} - 4e^{\beta/2} - 3\beta^2 + 2\beta + 2 + 2e^{-\beta})$

where the derivative is to be evaluated at the ordering temperature. This is valid provided one can ignore the fourth-order quadrupolar-magnetic coupling, which tends to be positive, and thus suppresses the ordering temperature. This term becomes more important at low T where the quadrupolar order is highly developed. Hence, if I_M is sufficiently large, the rapid growth of Q near the quadrupolar transition can significantly enhance the magnetic ordering tendencies, while if I_M is close to the critical value, the higher-order couplings cut in and suppress the tendency to magnetic order. This explains the increase in the critical magnetic coupling strength relative to the $I_Q=0$ limit.

B. Robustness of phase diagram

By examining the Landau theory, we can obtain some idea about the robustness of the phase diagram under the introduction of realistic fluctuation effects, specifically the quantum fluctuations induced by the Kondo effect, and the critical fluctuations in three dimensions.

Kondo effect. First, we note that the form of the free energy is fixed by symmetry considerations alone, as is always the case. Thus the introduction of the Kondo effect cannot modify the form of the free energy, merely modify the size of the coefficients.

Second, we note that the Kondo effect will have little effect on the magnitude of coefficients in the Landau free energy associated only with M , because the magnetism is van Vleck in character. Numerical studies of the single ion quadrupolar Kondo effect confirm that the van Vleck susceptibility is affected little in magnitude by the Kondo effect.⁶ However, it does acquire stronger temperature dependence than in the ionic limit, which will modify in detail the position of various features in the phase diagram and the temperature dependence of M in the ordered phase. In particular, the single ion susceptibility χ_{mag} due to van Vleck terms is expected to acquire upward curvature of the form¹⁵

$$\chi(T) \approx \chi(0)(1 - A\sqrt{T/T_K}), \quad (23)$$

where $\chi(0)$ is the zero-temperature limit, to within an order of unity the same as in the absence of the Kondo effect, T_K is the Kondo temperature, and A is a number of order unity. This gives a very shallow rise to the temperature T_M at which α_M changes sign. In contrast to the behavior for $T_K=0$ which, upon solving for $\alpha_M=0$ gives

$$T_M \approx \frac{\Delta}{\ln[1.5\Delta/(|I_M| - \Delta)]}. \quad (24)$$

In contrast, for $T_K > 0$, we obtain for $T_M \ll T_K$

$$T_M \approx \frac{T_K}{A^2} \left[1 - \frac{\Delta}{|I_M|} \right]^2, \quad (25)$$

which is generically smaller than the $T_K=0$ result (given $T_K \ll \Delta$ to be likely) and produces an increase of T_M with zero slope (as opposed to infinite for $T_K=0$). On the other hand, for $T_M \gg \Delta$, the Curie law form must return to the magnetic susceptibility, with no distinction

between $T_K=0$ and $T_K > 0$ cases. Thus for large coupling, the curve must match onto that of the $T_K=0$ calculations. Since the first-order phase boundary depends upon identifying a change of sign in β_M , for $I_Q=0$ we cannot safely say the magnetic phase boundary will retain its topology.

Third, we inquire about the influence of the Kondo effect on the terms involving Q . When the $1/T$ factor appears in our expressions in the table, that corresponds to the Curie law susceptibility of the ionic quadrupole moment. This will still apply should the intersite coupling greatly exceed the Kondo temperature, since then each ion yields a Curie law quadrupolar susceptibility. To handle, roughly, the case where $I_Q \leq T_K$, in the simplest possible approximation which captures the competition between the intersite coupling and the quantum fluctuations of the Kondo effect,¹⁸ we simply use the single-site partition function for one quadrupolar Kondo ion in the presence of the molecular field. This means all the Curie law β factors in the table will be replaced by the $\ln(T_K/T)/2\pi^2 T_K$ (Ref. 19) form expected for the quadrupolar Kondo effect. Solving for the second-order quadrupolar transition temperature T_Q by setting $\alpha_q=0$ where we replace the Curie law with the above expression, we see that it is never zero, and is given by

$$T_Q \approx T_K \exp(-2\pi^2 T_K / I_Q), \quad (26)$$

which, while smaller than the noninteracting value I_Q , always intersects the curve for T_M .

The structure of the phase diagram near the tricritical point for nonzero J_q appears essentially due to the terms $\delta_{mq} \bar{m}^2 \bar{q}$ and $\epsilon_{mq} \bar{m}^2 \bar{q}^2$ in the free energy, Eq. (16), generated by the Hamiltonian (12). Gufan *et al.*²⁰ using Landau's mean-field theory have analyzed the phase diagram of a free energy of the form given by (20), and they also found the same topology we have around the multicritical points. Those terms in our model are always present as long as we have ferroquadrupolar coupling and the hexagonal symmetry.

To summarize these considerations, then, we anticipate for large couplings $I_M \gg \Delta$, $I_Q \gg T_K$, the phase diagram will be unaltered by the Kondo effect. For I_M, I_Q comparable to Δ, T_K , the tendency to magnetic and quadrupolar line will still intersect the second-order magnetic line, we anticipate the same tricritical behavior and critical end point as seen without the Kondo effect. We cannot say without further calculation what will happen to the phase diagram in the absence of quadrupolar coupling.

Critical fluctuations. One might be concerned that critical fluctuations should alter the topology of the phase diagram and possibly the order of the transitions. We believe that this is not the case. First, critical fluctuations will certainly suppress all the ordering temperatures, but this is expected and generic. Second, critical fluctuations will certainly change the critical exponents at the second-order quadrupolar boundary in the phase diagram from mean-field values, but as long as that transition is ferroquadrupolar, they should not alter the order of the transition. Third, since the tricritical point occurs in the quadrupolar ordered phase, it is essentially magnetic in

character, i.e., it is derived from the magnetic order parameter alone. It is well-known that for a one-component order parameter, three dimensions is the lower critical dimension for the tricritical point, so that fluctuations, apart from reducing the ordering temperature, serve to induce logarithmic corrections to critical quantities. Such logarithmic corrections are difficult to detect. Fourth, we anticipate that the inclusion of the Kondo effect will enhance the applicability of the mean-field theory. This is because all critical temperatures are suppressed by the Kondo effect to much lower values (unless the couplings are quite strong). As the temperature is driven to zero, the dimensionality heads toward $3+1$ from the growth of the imaginary-time axis. Thus, the width of the critical regime must shrink.

The one possible downfall to the scenario in the previous paragraph is if the real magnetic order accesses multiple \mathbf{q} values, i.e., corresponds to ordered phases in which the possible order parameter transforms as a large space-group representation, rather than the single \mathbf{q} structure taken here. As has been extensively discussed in the context of the ϵ expansion,¹⁷ this situation may produce fluctuation induced first-order transitions. This cannot be ruled out by our simple considerations, and remains a subject for further investigations.

V. SUMMARY AND CONCLUSIONS

We have calculated the phase diagram of a simple model which includes intersite quadrupolar coupling between uranium ions in the hexagonal lattice. The model has some of the physics found in the hexagonal uranium-based materials, like the in-plane van Vleck magnetism, magnetic character along the c axis and degree of freedom to allow the possibility of quadrupolar-Kondo effect. We have shown that the intersite quadrupolar coupling between uranium ions enhances the critical temperature and plays the fundamental role in defining the nature of the transitions in the phase diagram. We have argued that the inclusion of the Kondo effect and critical fluctuations are unlikely to alter the essential structure of the phase diagram, provided $I_Q \neq 0$, but acknowledge that multiple \mathbf{q} ordering can, in principle, alter these conclusions. We intend to explore these issues further.

We now briefly explore the potential relevance of our study to the uranium based heavy-electron materials.

Based on the magnitudes of the specific-heat jumps and the magnetic moment \bar{m} given by the model around the tricritical point (TP) when J_q is of order $|J_m|/10$, we speculate this region as most probable to find the hexagonal doped compounds UPt_3 derived compounds $\text{U}(\text{Pt}_{1-y}, \text{Pd}_y)_3$ and $(\text{U}_{1-x}\text{Th}_x)\text{Pt}_3$ when $x, y \approx 0.05$. We are performing a model calculation based on the Coqblin-Schrieffer²¹ formalism to determine whether this coupling constant ratio can be realized in practice. We speculate that the phase diagram of UPd_2Al_3 (Ref. 9) might be understood by assuming the magnetic coupling to be in the region between the tricritical point and the critical end point. In this case, the higher-temperature transition would be quadrupolar, and the lower-temperature one antiferromagnetic and first order. Finally, the same kind of modeling can, in principle, apply to URu_2Si_2 due to the similarity of the ground non-Kramers doublets in hexagonal and tetragonal symmetry. However, the neutron Bragg peaks in that material correspond to a cell doubling along the c direction, so that a ferroquadrupolar ordering is unrealistic. Because of this, it is impossible to construct a third-order invariant in the free energy which couples the presumed quadrupolar order parameter to a single magnetic order parameter. Hence, the mechanism for enhancing the magnetic transition temperature and producing a magnetic tricritical point is eliminated, so that only a second-order quadrupolar transition would be likely.

In addition to this exploration of how the Kondo effect and critical fluctuation effects modify our already interesting results, we would like to explore the effects of magnetic field through magnetorestrictive coupling to see whether we can understand the metamagnetic transition observed in pure UPt_3 below 20 K in fields of order 20 T.²² Sharp metamagnetic transitions have also been observed in UPt_2Al_3 .⁹

ACKNOWLEDGMENTS

We acknowledge useful discussions with T.-L. Ho, C. Jayaprakash, M. Makivic, and J. W. Wilkins. We thank M. Alouani and R. MacKenzie for critical readings of the manuscript. V.L.L. was supported by Brazilian Council for Scientific and Technological Development (CNPq), and by University of São Paulo (USP). This research was supported by U.S. Department of Energy, Office of Basic Energy Sciences, Division of Materials Research.

¹C. Broholm, H. Lin, P. T. Matthews, T. E. Mason, W. J. L. Buyers, M. F. Collins, A. A. Menovsky, J. A. Mydosh, and J. K. Kjems, *Phys. Rev. B* **43**, 12 809 (1991).

²Y. Miyakko, S. Kawarazaki, H. Amitsuka, C. C. Paulsen, and K. Hasselbach, *J. Appl. Phys.* **70**, 5791 (1991).

³A. P. Ramirez, P. Coleman, P. Chandra, E. Bruck, A. A. Menovsky, Z. Fisk, and E. Bucher, *Phys. Rev. Lett.* **68**, 2680 (1992).

⁴Y. Miyako, H. Amitsuka, S. Kunii, and T. Kasuya, *Physica B*

(to be published).

⁵K. Asayama, Y. Kitaoka, and Y. Kohori, *J. Magn. Magn. Mater.* **76&77**, 449 (1988).

⁶D. L. Cox, *Phys. Rev. Lett.* **57**, 1240 (1987); *Physica B* (to be published).

⁷C. L. Seaman, M. B. Maple, B. W. Lee, S. Ghamaty, M. S. Torikachvili, J. S. Kang, L. Z. Liu, J. W. Allen, and D. L. Cox, *Phys. Rev. Lett.* **67**, 2882 (1991); see also B. Andraka and A. Tselik, *Phys. Lett.* **67**, 2887 (1991).

- ⁸H. Amitsuka, T. Hidano, T. Homma, H. Mitamura, and T. Sakikabara, *Physica B* (to be published).
- ⁹C. Geibel *et al.*, *Z. Phys B* **83**, 305 (1991); **84**, 1 (1991).
- ¹⁰S. J. Allen, *Phys. Rev.* **167**, 492 (1968).
- ¹¹M. Blume, V. Emery, and R. B. Griffiths, *Phys. Rev. A* **4**, 1071 (1971).
- ¹²K. W. H. Stevens, *Proc. Phys. Soc. A* **65**, 209 (1952).
- ¹³W. Hoston and A. N. Berker, *Phys. Rev. Lett.* **67**, 1027 (1991).
- ¹⁴A. I. Goldman, G. Shirane, G. Aeppli, B. Batlogg, and E. Bucher, *Phys. Rev. B* **34**, 6564 (1986).
- ¹⁵D. L. Cox (unpublished); D. L. Cox and A. Ruckenstein (unpublished).
- ¹⁶M. J. Stephen, E. Abrahams, and J. P. Straley, *Phys. Rev. B* **12**, 256 (1975).
- ¹⁷P. Bak and D. Mukamel, *Phys. Rev. B* **13**, 5086 (1976); D. Mukamel and S. Krinsky, *ibid.* **13**, 5076 (1976); S. J. Knak Jensen, O. G. Mouritsen, E. Kjaersgaard Hansen, and P. Bak, *ibid.* **19**, 5886 (1979).
- ¹⁸D. L. Cox, *Phys. Rev. B* **35**, 4561 (1987).
- ¹⁹P. D. Sacramento and P. Schlottmann, *Phys. Lett. A* **142**, 245 (1989); *Phys. Rev. B* **43**, 13 294 (1991).
- ²⁰Yu. M. Gufan and V. I. Torgashev, *Fiz. Tverd. Tela (Leningrad)* **22**, 1629 (1980) [*Sov. Phys. Solid State* **22**, 951 (1980)]; Yu. M. Gufan and E. S. Larin, *Fiz. Tverd. Tela (Leningrad)* **22**, 463 (1980) [*Sov. Phys. Solid State* **22**, 270 (1980)].
- ²¹B. Coqblin and J. R. Schieffer, *Phys. Rev.* **185**, 847 (1969); see also R. Siemann and B. Cooper, *Phys. Rev. Lett.* **44**, 1015 (1980).
- ²²J. J. M. Franse, P. H. Frings, A. de Visser, and A. Menovsky, *Physica B* **126**, 116 (1984).
- ²³P. D. Sacramento and P. Schlottmann, *Phys. Rev. B* **43**, 13 294 (1991).